Biogeosciences Discuss., doi:10.5194/bg-2016-199, 2016
Manuscript under review for journal Biogeosciences
Published: 29 June 2016

Biogeosciences Discussions
Open Access
EGU

Nitrogen oxides and ozone fluxes following organic and mineral fertilisation of a growing oilseed-rape

Raffaella M. Vuolo[1], Benjamin Loubet[1*], Nicolas Mascher[1], Jean-Christophe Gueudet[1], Brigitte Durand[1], Patricia Laville[1], Olivier Zurfluh[1], Raluca Ciuraru[1] and Ivonne Trebs[2]

1 UMR ECOSYS, INRA, AgroParisTech, Université Paris-Saclay, 78850, Thiverval-Grignon, France
2 Luxembourg Institute of Science and Technology (LIST), Environmental Research and Innovation (ERIN), 41, rue du Brill, L-4422 Belvaux, Luxembourg

* Corresponding author: Benjamin.Loubet@grignon.inra.fr

Abstract. This study reports NO, NO_2 and O_3 mixing ratios and flux measurements using the eddy-covariance method during a 7-months period over an oilseed rape field, spanning an organic and a mineral fertilisation event. Mean NO emissions during the whole period were in agreement with previous studies and showed quite small emissions of 0.26 kg N ha^{-1} with an emission factor of 0.27%, estimated as the ratio between total N emitted in form of NO and total N input. The NO emissions were higher following organic fertilisation in August due to conditions favouring nitrification (soil water content around 20% and high temperatures), while mineral fertilisation in February did not result in large emissions. The ozone (O_3) deposition velocity was significantly larger following organic fertilisation. We argue that reaction of O_3 with emitted NO or reaction of O_3 at the surface did not explain this finding, but we propose that reactions of O_3 with VOCs emitted by the slurry were the main reason. The analysis of the chemical and turbulent transport times showed that reactions between NO, NO_2 and O_3 below the measurement height occurred at all time during the 7-months period. Following organic fertilisation, the NO ground fluxes were 30% larger than the NO fluxes at the measurement height (3.2 m) , while the NO_2 fluxes changed sign during some periods, being negative at the surface and positive at the measurement height. This phenomenon of "apparent NO_2 emissions" reveals to be important during strong NO emissions and high O_3 ambient mixing ratios, even on a bare soil during August.

Keywords: eddy covariance, chemical reaction, transport time, oilseed rape, NO, O_3, NO_2

1. Introduction

Agricultural soils represent an important source of atmospheric nitric oxide (NO), especially in highly fertilized regions (Oikawa et al., 2015). Global estimates of total NO_x (NO + NO_2) emissions from soils range between 4 and 21 Tg N yr^{-1}, which represents between 10% and 15% of the global NO_x budget (Davidson and Kingerlee, 1997; Houghton et al., 2001; Yienger and Levy, 1995). NO_x, and especially NO_2, are toxic gases for humans (WHO, 2013) and national and international authorities regulate their levels. These inventories are subject to error in magnitude and especially in spatial distributions (Martin et al., 2003), which can be constrained by satellite observations, and ranges around 30% at the global scale (Toenges-Schuller et al., 2006). They are of considerable interest also for atmospheric photochemistry, and acting as ozone (O_3) precursors, they indirectly have an impact on climate. O_3 is a major tropospheric pollutant, harmful for humans and ecosystems, and is an important greenhouse gas, contributing to 25% of the anthropogenic net radiative forcing (Forster et al., 2007).

Biogeosciences Discuss., doi:10.5194/bg-2016-199, 2016
Manuscript under review for journal Biogeosciences
Published: 29 June 2016

NO_x emissions from soils are mostly due to nitrification and denitrification processes and through the chemical decomposition of HNO_2 (Laville et al., 2005; Meixner, 1997; Remde et al., 1989). Many authors emphasized that for most agricultural soils, nitrification is the dominant process of NO emissions (Bollmann et al., 1999; Dunfield and Knowles, 1999; Godde and Conrad, 2000). Organic and mineral fertilizers, rich in ammonium, increase NO emissions both by stimulating NO production by nitrification and by decreasing NO consumption.

There is a significant knowledge gap in understanding NO_x exchange between agricultural ecosystems and the atmosphere, partly due to a lack of direct measurements over long periods. NO emissions by soils can either be measured by dynamic chambers (Breuninger et al., 2012; Laville et al., 2009; Laville et al., 2011; Pape et al., 2009), aerodynamic gradient (Kramm et al., 1991), or eddy covariance methods (Rummel et al., 2002; Stella et al., 2013). Each method has its drawbacks and challenges: the dynamic chamber method may change the surface exchange parameters (Pape et al., 2009), and modify the fluxes due to fast reactions between the triad O_3-NO-NO_2, but thoroughly designed Teflon chambers can overcome this problem (Skiba et al., 2009). The aerodynamic gradient method (AGM) is nowadays applied for water-soluble compounds such as NH_3 (Milford et al., 2009), but has several biases of which flux divergence due to chemical reaction is the most limiting for NO-NO_2-O_3 (Duyzer et al., 1995; Kramm et al., 1991; Loubet et al., 2013). Non-stationarity and integration time is also limiting (Lenschow et al., 1994; Stella et al., 2012). The eddy covariance method is adapted for measuring NO fluxes. It is however also exposed to flux divergence issues due to NO-NO_2-O_3 chemical reactions. It is therefore essential to measure the fluxes and mixing ratios of the three compounds together.

The eddy covariance (EC) method is the state of the art flux measurement method for energy and CO_2 fluxes (Baldocchi, 2003), and due to the development of new analysers such as fast chemiluminescence, quantum cascade lasers absorption spectroscopy, or proton time of flight mass spectrometers (Ammann et al., 2012; Brodeur et al., 2009; Ferrara et al., 2012; Li et al., 2013; Muller et al., 2010b; Park et al., 2014; Peltola et al., 2014; Sintermann et al., 2011; Stella et al., 2013; Wolfe et al., 2009) it can nowadays be applied for several other trace gases. The main advantage of the EC method is that it is a "direct" measurement of the flux at a given height, which depends on fewer assumptions than the AGM, namely the Reynolds averaging and ergodicity hypothesis requiring that *the averaging time must be much larger than the time scales of variation of the air velocity* (Kaimal and Finnigan, 1994). This method has been successfully applied for measuring NO fluxes in a limited number of studies (Eugster and Hesterberg, 1996; Lee et al., 2015; Marr et al., 2013; Min et al., 2014; Rummel et al., 2002; Stella et al., 2013). The main difficulties of EC measurements are the high frequency losses due to adsorption to the tubing system, size of the absorption cell (Eugster and Senn, 1995) and differential advection caused by the radial variation of the mean velocity and simultaneous radial diffusion of the sample gas (Lenschow and Raupach, 1991). Moreover, since NO_2-to-NO photolytic converters typically applied in combination with chemiluminescence analysers have a conversion efficiency below 100%, measuring both NO and NO_2 with such a converter remains a challenge that requires to use two analysers simultaneously (Lee et al., 2015).

Due to these limitations, simultaneous measurements of NO, NO_2 and O_3 fluxes by eddy covariance have hence seldom been made. To our knowledge, only a few studies report such measurements and none over a crop. There is therefore a gap in knowledge as to whether NO, NO_2 and O_3 are interacting above crops and how nitrogen application will modify these fluxes and their interactions. Eugster and Senn (1995) report NO_2 fluxes by eddy covariance and analyse the errors of the method. Andreae et al. (2002) report comprehensive flux measurements

Biogeosciences Discuss., doi:10.5194/bg-2016-199, 2016
Manuscript under review for journal Biogeosciences
Published: 29 June 2016

in the Amazonian forest showing evidence of within forest cycling of the nitrogen oxides emitted from the soil. Horii et al. (2004) report NO_x and O_3 fluxes over a temperate deciduous forest showing consistent NO_x deposition. Ammann et al. (2012) report total reactive nitrogen fluxes by eddy covariance above grassland which compared well with dynamic chambers NO and NO_2 fluxes during periods with no NH_3 emissions. Geddes and Murphy (2014) report such measurements over two mixed hardwood forests in North America, under very low NO concentrations regime, which shows mainly NO_x deposition with evidence of chemical reactions in the canopy. Min et al. (2014) report such flux measurements over ponderosa pine which shows evidence of within canopy chemical removal of NO_x. Lee et al. (2015) and Marr et al. (2013) report fluxes of NO and NO_2 over urban areas which differ in their comparison with national emissions inventories: while Lee et al. (2015) found fluxes 80% larger than national inventories, the second study found similar fluxes but with large disagreements at the local scale.

In this study we are addressing the following science questions: (1) is the eddy covariance method adapted for quantifying the seasonal dynamics and diurnal cycles of the NO, NO_2 and O_3 fluxes above a crop rotation? (2) How are organic and mineral fertilisations affecting these fluxes and their dynamics? (3) To what extent are the chemical reactions between NO, NO_2 and O_3 modifying the fluxes above the ground? And finally, (4) why is O_3 deposition increasing following organic fertilisation? Is that a consequence of interactions with NO emissions?

For answering these questions we report measurements of NO, NO_2 and O_3 fluxes by eddy covariance using a system similar to Lee *et al.* (2015) for one month following slurry spreading over a bare soil at the FR-GRI fluxnet and ICOS site (Loubet et al., 2011). The NO and O_3 fluxes were measured over an additional further 6 month period to study the seasonality of these fluxes and to measure the fluxes following application of mineral fertiliser.

2. Materials and methods

2.1 Site description and management

The experiment took place in a 19 ha field located at Grignon (48°51' N, 1°58' E), 40 km west of Paris (France) and lasted more than 7 months from 07/08/2012 to 13/03/2013. The field was surrounded by heavy traffic roads on the east, south and south-west. The field belongs to a large farm (buildings at around 450 m to the south west) with around 210 dairy cows, 500 sheeps, and a production of approximately 900 lambs. The terrain has a gentle slope of ~1% and the mean annual temperature and precipitation are 10.9°C and 575 mm between 2005 and 2013. The main wind directions are north-west during clear days and southwest during cloudy and rainy days. The soil type is a *luvisol* or loamy clay (25% clay, 70% silt, 5% sand in the top 15 cm). The soil organic carbon content was ~20 g C kg^{-1}, pH (in water) = 7.6, and bulk soil density was 1.3 g m^{-3}. A detailed description of the site can be found in Laville et al. (2009; 2011), and Loubet et al. (2011).

The field was cultivated with winter wheat (a mix of Atlass and Premio species), which was harvested on 3 August 2012 (16.7 Mg ha^{-1} of dry matter). Cattle slurry was applied on the field with a trailing hose from the 18 to the 19 August 2012, at a rate of 42 kg N ha^{-1} of which 78% was ammonium (NH_4^+). The slurry had a very low dry matter content of 3.2% and a C/N ratio of 15.7. The total C applied was 666 kg C ha^{-1}. A gentle tillage was performed the 29 August 2012 to incorporate the crop and slurry residues and prepare the soil for oilseed rape sowing (variety Adriana) at a density of 35 plants per square meter. The crop developed slowly during the

Biogeosciences Discuss., doi:10.5194/bg-2016-199, 2016
Manuscript under review for journal Biogeosciences
Published: 29 June 2016

winter with a dry matter above ground (leaf area index) of 37 g m^{-2} (0.65 m^2 m^{-2}) the 25 October 2012 and 104 g m^{-2} (0.7 m^2 m^{-2}) the 18 February 2013. The canopy height stayed below 10 cm during the whole winter. Ammonium nitrate pellets were applied on oilseed rape the 20 February 2013 at a rate of 54 kg N ha^{-1}. Two selective herbicides were applied on the 2 (Springbok: 200 g L^{-1} of Metazachlore and 200 g L^{-1} of DMTA-P at 3 L ha^{-1}) and 31 October 2012 (Devin / Cycloxydime: 100 g L^{-1} at 1 L ha^{-1}) which only destroyed the weeds. In Decembre 2012 antilimaces pellets were applied.

2.2 Micrometeorological and ancillary measurements

Meteorological measurements included wind speed, air and soil temperatures and humidity as well as rain fall, global, net and photosynthetic active radiation. The meteorological measurements were performed on a mast (3.17m high) near the centre of the field and close to the flux measurement site (Fig. 1). Soil was sampled ~monthly for water content, total nitrogen and mineral nitrogen analysis. Measurements are described in (Loubet et al., 2011) and will not be detailed here.

A simplified sketch of the EC measurement system is shown in Figure 1. Three-dimensional wind and temperature fluctuations were measured near the centre of the field at 3.17 m above ground by a sonic anemometer (Gill R3 3-axis anemometer, Gill Instruments Limited, UK). A fast response open-path CO_2/H_2O infrared gas analyser (IRGA LI-7500A, LI-COR, USA) installed in a lateral distance of around 0.2 m to the sonic path measured CO_2 and H_2O fluctuations. O_3 mixing ratios were measured by a high-frequency, dry chemiluminescence O_3 detector (NOAA, USA) and its Teflon PFA inlet tube (length = 2.8 m, internal diameter = 0.32 mm) was positioned in between the sonic path and the IRGA at a lower height. The high-frequency signals were recorded at 20 Hz by Labview program developed in the laboratory. In accordance with (Lee et al., 2015), high-frequency (10 Hz) time series of NO and NO_2 were determined by two fast-response and closed-path chemiluminescence NO analysers (CLD 780TR, EcoPhysics, Switzerland), one being coupled to a photolytic converter (blue light converter, BLC, Droplet Measurement Technologies Inc, USA) for the detection of NO_2 (see Figure 1). The horizontal separation of the trace gas inlets from the sonic path was 20 cm. Air was sampled through two heated and shaded PFA tubes with a length of 20 m and an inner diameter of 9.55 mm. The first CLD was used for measuring NO and the second one connected to the BLC was used for detecting NO_2. Conversion efficiencies for NO_2 to NO of around 30% were achieved. The high-frequency signals of NO, NO_2 and O_3 were calibrated with mixing ratios measured at 30 min time resolution by slow-response analysers (ThermoScientific, Waltham, USA) (Figure 1). These instruments were calibrated every 3 to 6 weeks using the gas-phase titration (GPT) method and a 17 ppm NO standard (Air Liquide, FR). The fetch of the field site extended at least to 150 m in all directions and a footprint analysis showed that 90% of the time the entire field was in the footprint during neutral and moderately stable or unstable conditions (Loubet et al., 2011). NO and O_3 fast sensors were functioning during the whole campaign (07/08/2013 to 13/03/2013) together with NO, NO_2 and O_3 slow-response analysers and meteorological station. High frequency NO_2 measurement was performed from 14/08/2012 to 30/09/2012. In this study we focus on two periods: (1) from 14/08/12 to 29/08/12 during which all fluxes were measured and NO fluxes were the highest in order to investigate the interactions between the fluxes and mixing ratios of the NO-NO_2-O_3 triad, and (2) over the whole period for NO fluxes analysis. **[INSERT FIGURE 1]**

Biogeosciences Discuss., doi:10.5194/bg-2016-199, 2016
Manuscript under review for journal Biogeosciences
Published: 29 June 2016

2.3 Eddy covariance fluxes computations

The turbulent fluxes were computed as the covariance between the fluctuations of the scalar of interest and the vertical component of the wind. As the EC method and its theoretical background are described in the literature - e.g. (Foken, 2008) - details will not be provided here.

For closed-path sensors (NO, NO_2 and O_3), the lag time between w' and the dry mole fraction χ, had to be determined. This was done by searching for the maximum of the covariance function ($\overline{w'(t)\chi'(t-lag)}$). The lag for NO was 3.1 s [2.4-3.65 s] (Q50 [Q25-Q75]), for NO_2 it was 4.0 s [3.65-4.55 s], and for O_3 it was 2.9 s [2.5-3.25 s]. The lag was filtered for outliers and the covariance was computed as the value of the covariance function at the filtered lag.

As fast-response sensors for NO, NO_2 and O_3 were not absolute, the fluxes were computed following the ratio method for O_3 described by (Muller et al., 2010a), and in accordance with (Lee et al., 2015) for NO and NO_2:

$$F_{O3} = \overline{\chi_{O3}} \frac{\overline{w's'_{O3}}}{\overline{s_{O3}} v_d} \quad (1)$$

$$F_{NO} = \frac{\overline{w's'_{NO}}}{s_{NO} v_d} \quad (2)$$

$$F_{NO} = \frac{1}{\alpha v_d} \left(\frac{\overline{w's'_{NO2}}}{s_{NO2}} - \frac{\overline{w's'_{NO}}}{s_{NO}} \right) \quad (3)$$

where s_{O3} is the uncalibrated fast O_3 sensor signal (in mV) and χ_{O3} is the 30 min average of the slow-sensor reference O_3 mixing ratio (in ppb). Similarly s_{NO} and s_{NO2} are the fast NO and NO_2 sensor signals (in counts s^{-1}), while S_{NO} and S_{NO2} are the sensitivity of the analysers (in ppb (s counts)$^{-1}$). α is the blue light converter conversion efficiency, and v_d is the molar volume of dry air. All fluxes (momentum, heat, CO_2, H_2O, NO, NO_2, O_3) were computed by the Eddypro software and final flux data were averaged for 30 min intervals. Evaluation methodologies from the CarboEurope project were applied - see (Aubinet et al., 2000 ; Loubet et al., 2011).

2.4 Spectral corrections

Spectral attenuation of the flux is due to differential transport time of the compound in the tube and interaction with tube walls and filter surfaces (Massman and Ibrom, 2008). We tend to minimize this effect by insuring a large flow rate in the tubes with Reynolds number well above the critical threshold for turbulence - see (Lenschow and Raupach, 1991) - as well as heating the tubes to around 5°C above ambient temperature. The residence time of the air samples inside the tubing was around 1 s, ensuring low chemical conversions and the Reynolds number was 11700, hence largely in the turbulent range. However, water vapour interaction is still expected, and sensor separation also generates high frequency losses.

2.5 Estimation of the instrument and flux uncertainties

The NO, NO_2 and O_3 random instrument noises were estimated as the 1-σ random uncertainty of the signals as in Lenschow (2000), Langford et al. (2015) and Mauder et al. (2008). This noise is assumed to be "white" and hence uncorrelated to itself apart at lag = 0. It is therefore estimated as the difference between the autocorrelation at lag = 0 s and at lag = ± 0.05 s. The flux random uncertainty was itself evaluated as the covariance detection limit. It was determined as the root mean square error of the covariance function over 60 second periods at lag

Biogeosciences Discuss., doi:10.5194/bg-2016-199, 2016
Manuscript under review for journal Biogeosciences
Published: 29 June 2016

times well away from the position of the time lag. In practice, these were taken at lags larger than 120 s as absolute value as proposed by Langford et al. (2015).

2.6 Chemical reactions in the NO-NO_2-O_3 triad and effect on flux

The main gas phase reactions for the NO-O_3-NO_2 triad in the troposphere are (Seinfeld and Pandis, 2016):

$$NO + O_3 \rightarrow NO_2 + O_2 \qquad [k_r] \tag{R1}$$

$$NO_2 + O_2 + h\nu \rightarrow NO + O_3 \quad [J_{NO2}] \tag{R2}$$

Where $k_r = 0.0444 \exp(-1370 / (Ta + 273.15))$ in $ppb^{-1}\ s^{-1}$, and J_{NO2}, in s^{-1} is the photolysis frequency, which was retrieved as a function of global radiation R_g in $W\ m^{-2}$, $J_{NO2} = B1\ R_g + B2\ R_g$, following the approach of Trebs *et al*. (2009). The coefficients B1 and B2 were determined for our site by fitting measured data of global radiation and photolysis frequency that were available for the summer period in year 2002 (June to September, half hourly data). The fit of our data (4 months of half-hourly measurements of R_g and J_{NO2} accounting for about 5600 data points) results in B1 and B2 1.51×10^{-5} and 6.85×10^{-9} $W^{-1}\ m^2\ s^{-1}$, respectively. However, in the troposphere, and especially in a polluted atmosphere as in this study (advection from the Paris area and the surrounding roads), reactions with peroxy- and hydroperoxy radicals may be as important as R1-R2 for NO and NO_2 chemistry, since peroxy radicals are abundant in the urban area of Paris (Michoud et al., 2012).

$$RO_2 + NO \rightarrow RO + NO_2 \tag{R3}$$

$$HO_2 + NO \rightarrow OH + NO_2 \tag{R4}$$

Considering only the (R1) and (R2) reactions, the production and destruction term for O_3 is given by:

$$Q = k_r\,[NO]\,[O_3] - J_{NO2}\,[NO_2] \tag{4}$$

If Q > 0, O_3 and NO are consumed and NO_2 is formed. If Q < 0 instead, the reaction (R2) dominates and O_3 and NO are produced while NO_2 is consumed. If Q = 0, the net production of NO_x or O_3 is zero and the reactions R1-R2 equilibrate each other. This equilibrium is defined by the Photo-Stationary State ratio (Trebs et al., 2012)) :

$$PSS = k_r\,[NO][O_3] / J_{NO2}[NO_2] \tag{5}$$

PSS is unity when Q is zero. If R3-R4 reactions occur, PSS ratio may deviate from unity during night time ($J_{NO2} = 0$), or when R3 and R4 reactions occur, or if the air mass is not at equilibrium with surface fluxes. The production/destruction term Q and the PSS were estimated for the measurement height.

2.7 Transport and chemical time scales

Transport and chemical time scales τ_{trans} and τ_{chem} were calculated as in (Stella et al., 2012):

$$\tau_{trans} = R_a(z) \times (z_m - z_0) + R_b \times (z_0 - z_{0'}) \approx R_a(z) \times (z_m - z_0) \tag{6}$$

$$R_a(z) = \frac{u(z)}{u_*^2} - \frac{\Psi_H\left(\frac{z}{L}\right) - \Psi_M\left(\frac{z}{L}\right)}{k u_*} \tag{7}$$

$$R_b = (B_{St} u_*)^{-1} \tag{8}$$

Biogeosciences Discuss., doi:10.5194/bg-2016-199, 2016
Manuscript under review for journal Biogeosciences
Published: 29 June 2016

Where R_a and R_b are the aerodynamic and quasi-laminar boundary layer resistances, Ψ_H and Ψ_M the integrated correction stability functions for heat and momentum, B_{St} the Stanton number for the gas considered, and z_0 and $z_{0,}$ the roughness height for momentum and scalar, respectively. The chemical time scale of the NO-NO_2-O_3 triad is given by Lenschow (1982):

$$\tau_{chem} = 2[J_{NO2}^2 + k_r^2\,([O_3] - [\mathrm{NO}])^2 \; + 2\; J_{NO2}\; k_r([O_3] + [\mathrm{NO}] + 2[NO_2])]^{-0.5} \quad (9)$$

3. Results and discussion

3.1 Uncertainty in NO, NO_2 and O_3 flux measurements

The two main uncertainties were the high frequency losses, which were estimated with the in-situ ogive method (Ammann et al., 2006), and amounted to 10% for O_3, 20% for NO and 30% for NO_2 on average over the August-September period (when all fluxes were measured, see Figure 2). As a bias, they can be corrected for, and this was performed in the following of this manuscript. **[INSERT FIGURE 2]**

A second major uncertainty on flux measurements was the random uncertainty which was lower than 20% in most cases for O_3, NO (and similar to H_2O) and around 30% to 40% for NO_2 (Figure 3). For NO and NO_2 the random uncertainties peaked during the morning traffic hour around 6:00-8:00 UTC, which is explained by the non-stationarity generated by the local traffic on the mixing ratios. Hence overall the eddy covariance method proved to be usable for measuring NO fluxes over part of the season with an overall uncertainty similar to H_2O. A higher uncertainty was found for NO_2 fluxes which were smaller than NO fluxes and resulted from a difference from two instruments and a relatively low conversion ratio from NO_2 to NO (30%). **[INSERT FIGURE 3]**

3.2 Meteorological conditions

Daily averages of the air temperatures decreased during the measurement period, starting from about 20°C in summer and reaching minima around -5°C from December to March. Daily averages of global radiation decreased from 250 W m^{-2} in August to around 0 W m^{-2} in December, back to around 150 W m^{-2} in the end of March (Fig. 4). Daily average of the relative humidity was around 65% in August and September, and it increased to about 85% for the rest of the period. The wettest period was between October and November, and cumulative rain was 319 mm over the 7 months, which is quite high. The prevailing wind direction was south-west while the most intense winds were observed from north and south (Fig. 5). Figure 5 also shows that wind regimes were quite different in summer and winter: prevailing wind directions during August and February were from south-west and north-east, respectively. Soil water content (SWC) ranged between 20% and 40% (volume) (Fig. 4), with a long period between October and January with values around 28% and increased further in January to 35%, with sharp decrease during some periods. **[INSERT FIGURE 4]**

3.3 Seasonal dynamics and diurnal cycles of the NO, NO_2 and O_3 fluxes above a crop rotation

3.3.1 Seasonal dynamics of NO-NO_2-O_3 mixing ratios

Average daily NO, NO_2 and O_3 mixing ratios were 3.6, 6.9 and 24.8 ppb, respectively. The NO and NO_2 mixing ratios were higher when winds blew from the East (Paris), while O_3 showed the opposite behaviour, which can

Biogeosciences Discuss., doi:10.5194/bg-2016-199, 2016
Manuscript under review for journal Biogeosciences
Published: 29 June 2016

be explained by depletion of O_3 by NO sources from the surrounding traffic (as shown in Fig. 5) and reactions R1-R2. Daily NO_2 / NO_x ratios were on average 66%, which is typical for traffic and urban pollution (Carslaw, 2005; Minoura and Ito, 2010), and ranged from 4% to 93% during the entire period. The NO_2 mixing ratio was significantly higher than the NO mixing ratios in August and early September, end of January and mid-February, and end of March. During sporadic episodes, NO peaks were of the same order or even higher than NO_2 peaks (Fig. 4). **[INSERT FIGURE 5]**

3.3.2 Seasonal dynamics of NO-NO_2-O_3 fluxes

The average NO fluxes were very small, except during a period of strong emission following organic fertilisation on two days in August (18-19/08/2012), with maximum daily average fluxes of around 1.5 nmol m^{-2} s^{-1} (Fig. 4). Other emissions episodes, including mineral fertilisation in February (20/02/2013), were characterized by mean daily fluxes below 0.5 nmol m^{-2} s^{-1}. The NO fluxes were slightly negative part of the time (Q25, Q50 and Q75 equal -0.013, 0.031 and 0.11 nmol m^{-2} s^{-1}, Fig. 6). The O_3 fluxes ranged between -13.8 and 0 nmol m^{-2} s^{-1}, and averaged to -3.12 nmol m^{-2} s^{-1}. The largest O_3 deposition fluxes were observed following organic fertilisation in August, and were correlated with the strongest NO emissions. This period also corresponded to large daily O_3 mixing ratios (Fig. 4). The NO_2 fluxes were only measured during the first one and a half months (16 August to 30 September 2012) and were mostly negative (deposition), except during the first week following organic fertilisation (Q25, Q50 and Q75 equal -0.11, -0.07 and 0.08 nmol m^{-2} s^{-1})(Fig. 6). **[INSERT FIGURE 6]**

3.3.3 Diurnal cycles of mixing ratios and fluxes

O_3 mixing ratios exhibited a typical diurnal cycle that was governed by photochemistry and convective mixing within the boundary layer and from the free troposphere during daytime. It started to increase with sunlight around 7 a.m., and declined in the evening starting from 6 p.m. due to lack of photochemical formation in the absence of sunlight, deposition and destruction with NO in this high NO_x emission area. In general, NO mixing ratios featured a marked peak in the early morning and remained high until around 13:00 UTC (Fig. 7). During the early afternoon, the O_3 increase was correlated with the NO decrease. NO_2 mixing ratios showed a bi-modal diurnal cycle with its maxima in correspondence with morning and evening traffic peaks, i.e. around 6 a.m. and 7 p.m.

The NO fluxes also showed a diurnal cycle similar to the one of soil temperature with an emission peak around 12 a.m. (Fig. 7a and b). This suggests that NO emissions are related to nitrification, for which the emission rate is an exponential function of soil temperature (Henault et al., 2005). This was already shown for the Grignon soil by Laville *et al.* (2011). The fact that NO fluxes decrease earlier than soil temperature is most likely due to titration of NO by O_3 in the late morning and early afternoon, causing the NO emissions at the reference height to be reduced with respect to ground emissions. This is also indicated by the positive NO_2 flux observed during the same time of the day. The O_3 flux was mainly negative (deposition) and follows the diurnal dynamics of measured mixing ratios. **[INSERT FIGURE 7 and 7b]**

3.6 Influence of organic and mineral fertilisations on NO emissions

The NO flux averaged over the whole period was 0.09 nmol m^{-2} s^{-1} (mean), which is smaller than previous findings for the same site. Laville (2011) and Loubet et al. (2011) reported yearly averaged NO fluxes varying

Biogeosciences Discuss., doi:10.5194/bg-2016-199, 2016
Manuscript under review for journal Biogeosciences
Published: 29 June 2016

between 0.07 and 0.15 nmol m^{-2} s^{-1} for 2007-2009. The NO flux distribution was shifted towards positive values after the organic fertilisation in August (Fig. 6), with the mean NO flux during the two weeks following the fertilisation (0.49 nmol m^{-2} s^{-1}) being six times larger than over the whole period. Following the February mineral fertilisation the NO flux increased less and was only 1.7 larger than over the whole period (0.14 nmol m^{-2} s^{-1}). These numbers are also in line with those reported following fertilisation on the same soil in the 2007-2009 period by Laville (2011), Loubet et al. (2011), which also showed some periods with slightly negative NO fluxes. Stella et al. (2012) measured larger peak of NO emissions following slurry spreading, but these emissions lasted only two to three days, which was probably due to a dryer soil in this study.

Following the slurry application, the NO emissions amounted to 0.1 kg N ha^{-1}, which represents 0.25% of the applied nitrogen. Following the mineral fertilisation, the NO emissions amounted to 0.02 kg N ha^{-1}, which represents 0.037% of the applied nitrogen. On average, the NO emissions corresponded to 0.27% and 0.037% of the applied organic and mineral fertilizers (42 and 54 kg N), respectively. Over the whole period from August 2012 to March 2013, we evaluate a loss of 0.26 kg N ha^{-1}. With a total N input of 96 kg N ha^{-1}, this gives an estimate of the NO emission factor of 0.27%, which is similar to values reported earlier (Laville et al., 2011).

The reasons for smaller emissions following winter mineral fertilisation than following summer manure application are manifold. Even if the amount of applied nitrogen was similar for the two cases (42 and 54 kg N ha^{-1}), meteorological and soil conditions were much more favourable for nitrification in summer than in winter (Davidson, 1992; Williams and Fehsenfeld, 1991). Indeed, NO emissions from agricultural soils are mostly due to nitrification, and this hypothesis was tested for the Grignon site by Laville et al., (2011). Nitrification is inhibited by low soil temperature and high water content that causes anoxia. Soil temperature was much lower in February than in August (2.5 compared to 20 °C on average). February was particularly humid, with a total precipitation of 10 mm, while in August no significant rain event occurred after the first week, and the soil was only humidified by the organic manure supply (layer thickness of 4.8 mm) and occurred on a dry soil. The soil water content at 5 cm depth in September 2012 was around 21% in volume, while in February it was 33% in volume. These two factors led to more favourable conditions for nitrification in August than in February.

3.7 Chemical interactions: the NO-NO_2-O_3 triad and effect on the fluxes

In order to investigate the interactions between the fluxes and mixing ratios of the NO-NO_2-O_3 triad, we focus on the period from 14/08/12 to 29/08/12, during which all fluxes were measured and NO fluxes were the highest.

The two weeks following the organic manure application (from 18/08 to 19/08) are characterized by hot sunny days, with maximal global radiation above 800 W m^{-2}, except for the 24 August when the only rain event occurred (Fig. 8). The period of 18 to 23 August was warmest, with soil surface temperatures above 40°C at noon during most of the days, while the air temperature decreased from around 35°C to around 20°C during the same period. The soil temperature at 5 cm depth followed the same trend, but with lower daily maximum and higher night-time minimum. Although, due to sensor breakdown the soil water content was not measured during this period. The small latent heat flux (LE) after the 19 August, (17 W m^{-2} on average between 19 and 31 August) the large sensible heat flux (60 W m^{-2} on average) and radiation (212 W m^{-2} on average) indicate that the soil humidity of the top soil layer was low. Hence, we assume that the SWC was probably close to the one

Biogeosciences Discuss., doi:10.5194/bg-2016-199, 2016
Manuscript under review for journal Biogeosciences
Published: 29 June 2016

measured in September (around 20 % in volume), which is ideal for nitrification to occur (Laville et al., 2011; Oswald et al., 2013). **[INSERT FIGURE 8]**

The 18/08 was the first day when NO emissions from the soil occurred. The emissions lasted around two weeks following the organic fertilisation (Fig. 4), during which the NO flux during daytime exceeded 0.5 nmol m^{-2} s^{-1}, peaking around 12 a.m. The nocturnal NO flux usually decreased to zero, except for the night of 25/08, characterized by strong winds (Fig. 7b and 8). The maximum of the NO emissions was 2.7 nmol m^{-2} s^{-1} observed six days after fertilisation on the 21/08.

The NO_2 flux was significantly different during the two weeks following organic manure application compared to the period before (Fig. 7b and 8). It was in general positive during the day and around zero at night during the period 18/08 to 29/08, except for the night of the 25/08 when it was large and negative. Positive NO_2 fluxes might be explained by chemical reactions between NO and O_3 in the surface layer (De Arellano et al., 1993), which will be discussed in the next section.

The O_3 flux was also significantly higher following organic fertilisation than during the rest of the experimental campaign (Fig. 6). Since the mixing ratio of O_3 was quite variable during the campaign (Fig. 4), it is more interesting to look at the deposition velocity which underpins the surface exchange processes (Fig. 7b and 8). The median V_{dO3} during the organic fertilisation event exceeded the median over the rest of the experimental campaign by a factor of two. However, this increase in O_3 deposition velocity cannot be explained by reaction with soil emitted NO alone as the O_3 flux is an order of magnitude larger than the NO flux.

Different pathways for the near-surface O_3 removal are likely: i) photolysis of O_3 by ultraviolet light in the presence of water vapor forming OH radicals, ii) gas phase reactions with reactive VOCs and iii) heterogeneous reactions on soil or with adsorbed molecules on soil.

Around 60 % of BVOCs consists of very reactive terpenes, which may decrease the O_3 levels by chemical reactions. Reactive VOCs such as sesquiterpenes and monoterpenes were previously found to be emitted from soils (Horvath et al., 2012; Penuelas et al., 2014), and some of these sesquiterpenes species react with O_3 in the order of a few seconds. The reactions of O_3 with larger terpenes are important sources of OH, as well as the ozonolysis of simpler unsaturated compounds. In addition, these reactions represent important sources of semi-volatile compounds and particulate matter in the atmosphere, generally known as secondary organic aerosols (Donahue et al., 2005).

The NO mixing ratio was well correlated with the NO flux, with a correlation coefficient of 40% for the two weeks following the organic fertilisation (excluding 24-25 August), while it was only 2% for the 7-months period. This suggests that, following fertilisation, the ambient NO levels were mainly due to local emissions. The NO_2 mixing ratio was less correlated with the NO_2 flux, suggesting that NO_2 levels were more related to advection from surrounding traffic roads than from local emissions. Indeed, both NO and NO_2 are emitted from traffic roads and urban pollution, but the NO_2 component quickly becomes prevalent as the plume is advected, especially in presence of high O_3 levels, as in our case (Carslaw, 2005; Minoura and Ito, 2010). The minimum night-time mixing ratio is mainly controlled by night-time wind velocity: the higher the night-time velocity, the higher the mixing ratio, due to a better mixing in the atmospheric surface layer. During conditions with lower wind speed, deposition and reaction with local NO_x sources lead to a high depletion of O_3 during the night. The maximum daily mixing ratio of ozone is controlled by radiation and temperature as well as a regional

Biogeosciences Discuss., doi:10.5194/bg-2016-199, 2016
Manuscript under review for journal Biogeosciences
Published: 29 June 2016

atmospheric loading of NO_x and VOCs, while the daily ozone deposition flux is controlled by friction velocity and stomatal aperture.

3.7.1 To what extent are the chemical reactions between NO, NO_2 and O_3 modifying the fluxes above the ground?

Measured mixing ratios and fluxes of NO, NO_2 and O_3 are affected by chemical reactions (R1 to R4) in addition to emissions and deposition processes. Especially, the diurnal fluxes of NO_2 observed from the 18 to the 23 August, were positive (emissions) and of the same order of magnitude as the NO fluxes, while they were negative afterwards. The simultaneous observation of positive NO and NO_2 fluxes are typical for the NO-to-NO_2 transformation below the flux observation level in the presence of high O_3 mixing ratios. This phenomenon is called "apparent NO_2 emissions" and was observed in other studies mainly above dense or tall canopies (Ammann et al., 2012; Min et al., 2014; Plake et al., 2015). For the reaction (R1-R2) to occur below the measurement height, the turbulent transport time (τ_{trans}) needs to exceed the chemical reaction time (τ_{chem}) (Arellano and Duynkerke, 1992; De Arellano et al., 1993; Lenschow and Delany, 1987; Plake et al., 2015; Stella et al., 2013; Stella et al., 2011; Stella et al., 2012). The Damköhler number $Da = \tau_{trans} / \tau_{chem}$ is often used to determine the conditions favourable for chemical reactions: in cases when Da is higher than unity chemical reactions are significantly faster than the transport (flux divergence), whereas values for Da smaller than 0.1 indicates that the influence of chemical reactions was negligible. The aerodynamic resistance $R_a(z)$ (Eq. 7) was overall quite small and ranging from 45 to 128 s m^{-1} (1st and 3rd quantiles), hence leading to a quite short transport time scale (larger than 100 s most of the time). The boundary layer resistance was around 22 and 43 s m^{-1} (1st and 3rd quantiles) for O_3 (Fig. 9). The surface resistance for O_3 was estimated as $R_{soil}(O_3) = V_{dO3}^{-1} - R_a - R_b(O_3)$, and dominated the other resistances (100 to 480 s m^{-1}). The O_3 penetration depth in the soil was estimated as the depth necessary to explain the measured $R_{soil}(O_3)$ if molecular diffusion drives transfer in the soil. In practice this corresponded to the dry soil layer used in (Personne et al., 2009). This depth ranged from 2 to 10 mm on average and was smaller at noon than during the night (Fig. 9). Overall, the chemical time τ_{chem} and the transport time τ_{trans} were of the same order of magnitude at any time of the day between applications and during mineral fertilisation, and τ_{chem} was smaller than τ_{trans} during the organic fertilisation. As a consequence, the Damköhler number was around unity most of the time and larger than unity during the organic fertilisation period, showing that reaction between O_3, NO and NO_2 happened during transport from the ground to the mast at all times at this site. During the fertilisation event, the Damköhler number was especially high at night, when the transport time increased more substantially than the chemical timescale. These results are similar to findings by Stella et al. (2012) for the same site over bare soil. During the periods with vegetation, the increase of the transport was less than of the chemical time scale during nighttime, as the presence of vegetation increases the mixing, and, hence diminishes $R_a(z)$. **[INSERT FIGURE 9]**

The Damköhler number shows that NO reacts with O_3 and that photolysis also plays a role. How does this affect the NO flux measured at the reference height compared to the one at the ground? Based on the early developments of Lenschow (1982) and Lenschow and Delany (1987), a method was developed by Duyzer et al. (1995) to compute the flux at the ground based on the measured flux at the reference height. This method assumes a logarithmic profile of the flux divergence and depends on measured mixing ratios, stability function and friction velocity:

Biogeosciences Discuss., doi:10.5194/bg-2016-199, 2016
Manuscript under review for journal Biogeosciences
Published: 29 June 2016

$$(\partial F/\partial z)_z = a \ln z + b \quad (10)$$

$$a_{NO_2} = -a_{NO} = -a_{O_3} = -\Phi_H / ku_* \left[k_r \left(\overline{[NO]} F_{O_3,z_{ref}} + \overline{[O_3]} F_{NO,z_{ref}}\right) - j_{NO_2} F_{NO_2,z_{ref}}\right] \quad (11)$$

Here $\overline{[NO]}$ and $\overline{[O_3]}$ are mixing ratios which should ideally refer to the geometric mean height of the profile measurements but was taken from the measurement height in our study, z_{ref} is the measurement height and Φ_H is the stability correction function for heat estimated at z_{ref} (Dyer and Hicks, 1970). Coefficient b of Eq. 10 can be computed as $b = -a \ln(z_2)$ where z_2 is the height above which the flux divergence is zero. Duyzer et al. (1995) showed with numerical simulations that the NO_x flux divergence could be approximated by Eq. 10 below a height of 4m, while it was negligible above. We refer to 4 m as the reference height z_2 at which we assume the flux divergence to be zero. Equation 10 can be integrated from measurement height to any height, for each compound giving:

$$F(z_{z0}) = F(z_{ref}) + a(1 + \ln(z_2))(z_{ref} - z_0) - a[z_{ref} \ln(z_{ref}) - z_0 \ln(z_0)] \quad (12)$$

[INSERT FIGURE 10]

Mainly due to the reaction with O_3, the calculated NO flux at the ground surface was on average 32% larger than that at the measurement height during the period 17-29/08 (0.93 instead of 0.63 nmol m^{-2} s^{-1}). This would represent an increase of 37 g N emission following slurry spreading. For NO_2, the calculated flux at the ground surface was mostly negative while it was mainly positive at the reference height during the period 18-22/08. On average the NO_2 flux at the ground was -0.33 nmol m^{-2} s^{-1} over the period 17-29/08 while it was -0.03 nmol m^{-2} s^{-1} at the reference height. For NO fluxes, the major discrepancy between fluxes at the surface and the measurement height occurs during periods with relatively large and stable values of the Damköhler number (Fig. 10), as this is the case when chemical reactions consume NO before it reaches the measurement height.

Since the O_3 deposition flux was much larger than the NO flux, the reaction with NO changed the absolute value by only 3% when comparing the flux at the measurement height to the ground surface. Indeed, as only reactions (R1) and (R2) are considered in eqs. (4) and (5), which we used to numerically evaluate surface fluxes, we obtain: $\Delta[FNO] = \Delta[F_{O_3}] = -\Delta[FNO_2] = 0.3$ nmol m^{-2} s^{-1} where Δ stands for the difference between surface and measurement height.

3.7.2 Why is O_3 deposition increasing following organic fertilisation?

We observed that following organic fertilisation O_3 deposition increased by a factor of two (as shown by the deposition velocity, Figs. 7 & 8). Although the reactions with NO during transport are shown to be small compared to the NO flux, reactions in the soil surface layer may be more important due to large NO concentrations in the soil, despite the fact that this layer is very small. This would, however, mean that the NO_2 produced in the soil would be adsorbed on the soil surface either on the mineral phase or dissolved the water phase as NO_2^-. To evaluate this assumption, we evaluated the Damköhler number in the soil surface layer, with few assumptions: (1) the layer depth is equal to the O_3 penetration depth δ_{O3soil} (Fig. 9), in this layer the transport time is equal to soil resistance for O_3 times the penetration depth $R_{soilO3} \times \delta_{O3soil}$. (2) The NO mixing ratio in this layer can be retrieved in a first instance assuming no chemical reaction in the atmosphere by making advantage

Biogeosciences Discuss., doi:10.5194/bg-2016-199, 2016
Manuscript under review for journal Biogeosciences
Published: 29 June 2016

of the resistance analogy: $[NO]_{soil} \approx [NO]_{ref} + F_{NO,z_{ref}} \times \left(R_a(z_{ref}) + R_{bNO} + R_{soilNO}\right)$. Assuming no chemical reaction in the surface layer would not change the magnitude of $[NO]_{soil}$ since, as shown in Figure 10, F_{NO,z_0} is of the same order of magnitude as $F_{NO,z_{ref}}$. In this equation, (3) R_{bNO} can be estimated as equal to $R_{bO3} \times D_{molO3} / D_{molNO}$, with $D_{molNO} = 1.8\ 10^{-5}$ m^2 s^{-1} and $D_{molO3} = 1.44\ 10^{-5}$ m^2 s^{-1}. Finally, (4) in the soil, the NO_2 photolysis constant can be assumed to be zero because radiation decreases sharply (although it may persist over a certain depth). This calculation results in Da ≤ 0.01, which means that reaction of O_3 with NO in the soil cannot explain the observed increase in O_3 flux following slurry application. On the other hand we can evaluate the NO mixing ratio that would explain the additional O_3 destruction at the surface, by searching for the value of $[NO]_{soil}$ that satisfies $\tau_{trans}(Soil, O_3) = \tau_{chem}(Soil, O_3)$. By doing so, we found that $[NO]_{soil}$ would need to reach 5 to 40 ppm to explain the increase in O_3 deposition following organic fertilisation. Gut *et al.* (1998) and Gut *et al.* (1999) measured NO mixing ratios at 2 cm depth in soil under wheat with the membrane tube technique and report mixing ratios around 100 ppb and always below 400 ppb following fertilisation, which is one order to two order of magnitude below the mixing ratio which would be needed to explain the observed O_3 flux. Moreover, the rate of NO production in the soil surface layer would have to be equal to the O_3 flux to the ground (around 20 nmol m^{-2} s^{-1}) which is an order of magnitude larger than what Gut *et al.* (1998) or Laville *et al.* (2009) report as maximum NO flux. Thus, we conclude that this mechanism of removal is very unlikely.

Currently, there is little or no data available on the emission of VOCs from slurry application. However, a recent study mainly focusing on quantification of odor emissions from soil application of manure slurry, shows the formation of a certain number of VOCs, included organic sulfur compounds, carboxylic acids, alcohols, carbonyl compounds (ketones and aldehydes), aromatic compounds (phenols and indoles) and nitrogen compounds (Feilberg et al., 2015). Based on their analyses, the compound most responsible for the overall odor impact from the VOC emissions was 4-methylphenol. The authors showed also the emission of trimethylamine, a compound that can react fast with O_3, leading to formation of secondary organic aerosols (Murphy et al., 2007). Furthermore, the authors suggest that a large part of these VOCs are formed through ozonation reactions (i.e. byproducts of ozonation: methanol, acetone, and acetaldehyde). Indeed, the slurry will be transported downwards through the soil, where efficient heterogeneous reactions can take place at particle interfaces. It has been shown that the heterogeneous reaction probabilities may be much greater than anticipated. For example, measurements on oxide surfaces with chemical structure commonly found in VOCs (i.e. alkenes, terpenes, carbonyls) showed that the O_3 reaction probability of a surface-attached alkene can be up to five orders of magnitude greater than for the same reaction in the gas-phase (Stokes et al., 2008). In the same way, Fick et al. (2005) observed that ozonolysis reaction rates of some terpenes were much higher than predicted, possibly as a result of reactions on the surfaces used in their experiments. These results suggest that terpenes can remain on the surfaces, enhancing the O_3 reactivity. Similarly, some other authors observed that surface reaction probabilities with O_3 were 10 to 120 times greater than their corresponding gas-phase values (Dubowski et al., 2004; Springs et al., 2011). It is also known that soils can act as a sink of VOCs, by their adsorption to soil mineral particle surfaces and humic substances (Penuelas et al., 2014). Hence, it is likely that surface chemistry including photo-enhanced O_3 uptake on organic matter (Jammoul et al., 2008; Reeser et al., 2009) may explain the increase in O_3 deposition, a process yet not described in the literature. It may also be likely that O_3 is destroyed by very reactive VOCs in the gas phase as hypothesized by Wolfe et al. (2011). These gas-phase

Biogeosciences Discuss., doi:10.5194/bg-2016-199, 2016
Manuscript under review for journal Biogeosciences
Published: 29 June 2016

reactions, however, require that the chemical reaction time to be shorter than the turbulence transport time (Plake et al., 2015; Stella et al., 2012).

4. Conclusions

Eddy covariance flux measurements of the NO-NO_2-O_3 triad during a 7 months period allowed evaluating several mechanisms controlling the exchange of these reactive trace gases with an agricultural soil. Eddy covariance technique revealed to be suitable to catch seasonal and diurnal dynamics of the fluxes, and allowed to interpret fluxes behaviour according to meteorological variables, fertilisation practices and chemical reactions. In particular, the magnitude and temporal variability of NO emission fluxes following two fertilisation episodes were analysed, one in summer and the other one in winter. Mean NO emissions during the whole period were in agreement with previous studies on the same site. Emissions were significantly higher (a factor of seven) during two weeks following organic fertilisation in August than during the rest of the experimental period. These large emissions are mainly due to favourable conditions for nitrification: soil water content around 20% and high temperatures. In February, following mineral fertilisation, the increase of NO emissions was less pronounced, although the same amount of N was applied. This difference is likely due to less favourable conditions for nitrification in February (low temperature and higher soil water content), rather than to the different form of fertilizer. On average over the whole period, we derived a loss of 0.26 kg N ha^{-1} as NO from the field. With a total N input of 96 kg N ha^{-1}, this results in an NO emission factor of 0.27%, which is on the lower range of earlier reported values on this site (Laville et al., 2011).

The O_3 deposition velocity was significantly larger following organic fertilisation than during the rest of the experiment, despite the fact that vegetation was absent. This increase in O_3 deposition could not be explained by reaction of O_3 with emitted NO as the NO flux was an order of magnitude smaller than that of O_3, nor could it likely be explained by reaction of NO at the surface. The process behind this increase is still to be discovered, but we hypothesize here that reactions of O_3 with VOCs emitted by the slurry were the main reason.

The evaluation of the chemical and turbulent transport times showed that reactions between NO, NO_2 and O_3 below the measurement height occurred during the whole measurement period, leading to a depletion of NO and a build-up of NO_2 from the ground to the measurement height. Following organic manure application, NO fluxes were reduced by 30% from the surface to measurement height, while the NO_2 fluxes changed sign, being negative at the surface and positive at the measurement height. This phenomenon of "apparent NO_2 emissions" was reported in other studies, especially above forests. Here it also reveals to be important above a bare soil and at moderate measurement heights, in conditions of strong NO emissions and high ambient O_3 mixing ratios.

Acknowledgements

This work was funded by the FP7 projects ECLAIRE (grant number 282910) and INGOS (grant agreement 284274), the French ANR project ANAEE (), as well as ICOS France. The authors acknowledge the director of the AgroParsiTech Farm Dominique Tristan for letting the access to the field. We are grateful to the Max Planck Institute for Chemistry (Mainz, Germany) for the loan of a CLD 780TR analyser during the time of the experiment.

Biogeosciences Discuss., doi:10.5194/bg-2016-199, 2016
Manuscript under review for journal Biogeosciences
Published: 29 June 2016

520 **References**

Ammann, C., Brunner, A., Spirig, C., and Neftel, A.: Technical note: Water vapour concentration and flux measurements with PTR-MS, Atmospheric Chemistry and Physics, 6, 4643-4651, 2006.

Ammann, C., Wolff, V., Marx, O., Bruemmer, C., and Neftel, A.: Measuring the biosphere-atmosphere exchange of total reactive nitrogen by eddy covariance, Biogeosciences, 9, 4247-4261, 2012.

525 Andreae, M. O., Artaxo, P., Brandao, C., Carswell, F. E., Ciccioli, P., da Costa, A. L., Culf, A. D., Esteves, J. L., Gash, J. H. C., Grace, J., Kabat, P., Lelieveld, J., Malhi, Y., Manzi, A. O., Meixner, F. X., Nobre, A. D., Nobre, C., Ruivo, M. D. L. P., Silva-Dias, M. A., Stefani, P., Valentini, R., von Jouanne, J., and Waterloo, M. J.: Biogeochemical cycling of carbon, water, energy, trace gases, and aerosols in Amazonia: The LBA-EUSTACH experiments, J. Geophys. Res.-Atmos., 107, 2002.

530 Arellano, J. and Duynkerke, P. G.: Influence of chemistry on the flux-gradient relationships for the NO-O3-NO2 system, Boundary-Layer Meteorology, 61, 375-387, 1992.

Aubinet, M., Grelle, A., Ibrom, A., Rannik, U., Moncrieff, J., Foken, T., Kowalski, A. S., Martin, P. H., Berbigier, P., Bernhofer, C., Clement, R., Elbers, J., Granier, A., Grunwald, T., Morgenstern, K., Pilegaard, K., Rebmann, C., Snijders, W., Valentini, R., and Vesala, T.: Estimates of the annual net carbon and water exchange

535 of forests: the EUROFLUX methodology, Advances in Ecological Research, 30, 113-175, 2000.

Baldocchi, D. D.: Assessing the eddy covariance technique for evaluating carbon dioxide exchange rates of ecosystems: past, present and future, Global Change Biology, 9, 479-492, 2003.

Bollmann, A., Koschorreck, M., Meuser, K., and Conrad, R.: Comparison of two different methods to measure nitric oxide turnover in soils, Biology and Fertility of Soils, 29, 104-110, 1999.

540 Breuninger, C., Oswald, R., Kesselmeier, J., and Meixner, F. X.: The dynamic chamber method: trace gas exchange fluxes (NO, NO2, O-3) between plants and the atmosphere in the laboratory and in the field, Atmos. Meas. Tech., 5, 955-989, 2012.

Brodeur, J. J., Warland, J. S., Staebler, R. M., and Wagner-Riddle, C.: Technical note: Laboratory evaluation of a tunable diode laser system for eddy covariance measurements of ammonia flux, Agricultural and Forest

545 Meteorology, 149, 385-391, 2009.

Carslaw, D. C.: Evidence of an increasing NO2/NOX emissions ratio from road traffic emissions, Atmospheric Environment, 39, 4793-4802, 2005.

Davidson, E. A.: Sources of Nitric-Oxide and Nitrous-Oxide Following Wetting of Dry Soil, Soil Sci Soc Am J, 56, 95-102, 1992.

550 Davidson, E. A. and Kingerlee, W.: A global inventory of nitric oxide emissions from soils, Nutrient Cycling in Agroecosystems, 48, 37-50, 1997.

De Arellano, J. V.-G., Duynkerke, P. G., and Builtjes, P. J. H.: The divergence of the turbulent diffusion flux in the surface layer due to chemical reactions: the NO-O3-NO2 system, Tellus B, 45, 23-33, 1993.

Donahue, N. M., Hartz, K. E. H., Chuong, B., Presto, A. A., Stanier, C. O., Rosenhorn, T., Robinson, A. L., and

555 Pandis, S. N.: Critical factors determining the variation in SOA yields from terpene ozonolysis: A combined experimental and computational study, Faraday Discussions, 130, 295-309, 2005.

Dubowski, Y., Vieceli, J., Tobias, D. J., Gomez, A., Lin, A., Nizkorodov, S. A., McIntire, T. M., and Finlayson-Pitts, B. J.: Interaction of gas-phase ozone at 296 K with unsaturated self-assembled monolayers: A new look at an old system, Journal of Physical Chemistry A, 108, 10473-10485, 2004.

Dunfield, P. F. and Knowles, R.: Nitrogen monoxide production and consumption in an organic soil, Biology and Fertility of Soils, 30, 153-159, 1999.

Duyzer, J. H., Deinum, G., and Baak, J.: The Interpretation of Measurements of Surface Exchange of Nitrogen-Oxides - Correction for Chemical-Reactions, Philos T R Soc A, 351, 231-248, 1995.

Dyer, A. J. and Hicks, B. B.: Flux-profile relationship in the constant flux layer, Q. J. Roy. Meteor. Soc., 96, 715-721, 1970.

Eugster, W. and Hesterberg, R.: Transfer resistances of NO2 determined from eddy correlation flux measurements over a litter meadow at a rural site on the Swiss plateau, Atmospheric Environment, 30, 1247-1254, 1996.

Eugster, W. and Senn, W.: A Cospectral Correction Model for Measurement of Turbulent No2 Flux, Boundary-Layer Meteorology, 74, 321-340, 1995.

Feilberg, A., Bildsoe, P., and Nyord, T.: Application of PTR-MS for Measuring Odorant Emissions from Soil Application of Manure Slurry, Sensors, 15, 1148-1167, 2015.

Ferrara, R. M., Loubet, B., Di Tommasi, P., Bertolini, T., Magliulo, V., Cellier, P., Eugster, W., and Rana, G.: Eddy covariance measurement of ammonia fluxes: Comparison of high frequency correction methodologies, Agricultural and Forest Meteorology, 158, 30-42, 2012.

Fick, J., Pommer, L., Astrand, A., Ostin, R., Nilsson, C., and Andersson, B.: Ozonolysis of monoterpenes in mechanical ventilation systems, Atmospheric Environment, 39, 6315-6325, 2005.

Foken, T.: The energy balance closure problem: An overview, Ecological Applications, 18, 1351-1367, 2008.

Forster, P., Ramaswamy, V., Artaxo, P., Berntsen, T., Betts, R., Fahey, D. W., Haywood, J., Lean, J., Lowe, D. C., Myhre, G., Nganga, J., Prinn, R., Raga, G., M., S., and Van Dorland, R.: Changes in Atmospheric Constituents and in Radiative Forcing. In: Climate Change 2007: The Physical Science Basis. Contribution of Working Group I to the Fourth Assessment Report of the Intergovernmental Panel on Climate Change Solomon, S., D. Qin, M. Manning, Z. Chen, M. Marquis, K.B. Averyt, M.Tignor and H.L. Miller (eds.) (Ed.), Cambridge University Press, Cambridge, United Kingdom and New York, NY, USA., 2007.

Geddes, J. A. and Murphy, J. G.: Observations of reactive nitrogen oxide fluxes by eddy covariance above two midlatitude North American mixed hardwood forests, Atmospheric Chemistry and Physics, 14, 2939-2957, 2014.

Godde, M. and Conrad, R.: Influence of soil properties on the turnover of nitric oxide and nitrous oxide by nitrification and denitrification at constant temperature and moisture, Biology and Fertility of Soils, 32, 120-128, 2000.

Gut, A., Blatter, A., Fahrni, M., Lehmann, B. E., Neftel, A., and Staffelbach, T.: A new membrane tube technique (METT) for continuous gas measurements in soils, Plant and Soil, 198, 79-88, 1998.

Gut, A., Neftel, A., Staffelbach, T., Riedo, M., and Lehmann, B. E.: Nitric oxide flux from soil during the growing season of wheat by continuous measurements of the NO soil-atmosphere concentration gradient: A process study, Plant and Soil, 216, 165-180, 1999.

Henault, C., Bizouard, F., Laville, P., Gabrielle, B., Nicoullaud, B., Germon, J. C., and Cellier, P.: Predicting in situ soil N2O emission using NOE algorithm and soil database, Global Change Biology, 11, 115-127, 2005.

Horii, C. V., Munger, J. W., Wofsy, S. C., Zahniser, M., Nelson, D., and McManus, J. B.: Fluxes of nitrogen oxides over a temperate deciduous forest, J. Geophys. Res.-Atmos., 109, 2004.

600 Horvath, E., Hoffer, A., Sebok, F., Dobolyi, C., Szoboszlay, S., Kriszt, B., and Gelencser, A.: Experimental evidence for direct sesquiterpene emission from soils, J Geophys Res-Atmos, 117, 2012.

Houghton, J. T., Y. Ding, D.J. Griggs, M. Noguer, P.J. van der Linden, X. Dai, K.Maskell, and Johnson, C. A.: IPCC, 2001: Climate Change 2001: The Scientific Basis. Contribution of Working Group I to the Third Assessment Report of the Intergovernmental Panel on Climate Change 881 pp., 2001.

605 Jammoul, A., Gligorovski, S., George, C., and D'Anna, B.: Photosensitized heterogeneous chemistry of ozone on organic films, Journal of Physical Chemistry A, 112, 1268-1276, 2008.

Kaimal, J. C. and Finnigan, J. J.: Atmospheric Boundary Layer Flows, Their structure and measurement., Oxford University Press., New York, 1994.

Kramm, G., Muller, H., Fowler, D., Hofken, K. D., Meixner, F. X., and Schaller, E.: A Modified Profile Method
610 for Determining the Vertical Fluxes of No, No2, Ozone, and Hno3 in the Atmospheric Surface-Layer, J Atmos Chem, 13, 265-288, 1991.

Langford, B., Acton, W., Ammann, C., Valach, A., and Nemitz, E.: Eddy-covariance data with low signal-to-noise ratio: time-lag determination, uncertainties and limit of detection, Atmos. Meas. Tech., 8, 4197-4213, 2015.

615 Laville, P., Flura, D., Gabrielle, B., Loubet, B., Fanucci, O., Rolland, M. N., and Cellier, P.: Characterisation of soil emissions of nitric oxide at field and laboratory scale using high resolution method, Atmospheric Environment, 43, 2648-2658, 2009.

Laville, P., Henault, C., Gabrielle, B., and Serca, D.: Measurement and modelling of NO fluxes on maize and wheat crops during their growing seasons: effect of crop management, Nutrient Cycling in Agroecosystems, 72,
620 159-171, 2005.

Laville, P., Lehuger, S., Loubet, B., Chaumartin, F., and Cellier, P.: Effect of management, climate and soil conditions on N2O and NO emissions from an arable crop rotation using high temporal resolution measurements, Agricultural and Forest Meteorology, 151, 228-240, 2011.

Lee, J. D., Helfter, C., Purvis, R. M., Beevers, S. D., Carslaw, D. C., Lewis, A. C., Moller, S. J., Tremper, A.,
625 Vaughan, A., and Nemitz, E. G.: Measurement of NOx Fluxes from a Tall Tower in Central London, UK and Comparison with Emissions Inventories, Environmental Science & Technology, 49, 1025-1034, 2015.

Lenschow, D. and Delany, A. C.: An analytic formulation for NO and NO2 flux profiles in the atmospheric surface layer, J Atmos Chem, 5, 301-309, 1987.

Lenschow, D. H.: Reactive trace species in the boundary layer from a micrometeorological perspective, Journal
630 of the Meteorological Society of Japan, 60, 472-480, 1982.

Lenschow, D. H., Mann, J., and Kristensen, L.: How Long Is Long Enough When Measuring Fluxes and Other Turbulence Statistics, Journal of Atmospheric and Oceanic Technology, 11, 661-673, 1994.

Lenschow, D. H. and Raupach, M. R.: The Attenuation of Fluctuations in Scalar Concentrations through Sampling Tubes, J Geophys Res-Atmos, 96, 15259-15268, 1991.

635 Lenschow, D. H., Wulfmeyer, V., and Senff, C.: Measuring second- through fourth-order moments in noisy data, J Atmos Ocean Tech, 17, 1330-1347, 2000.

Li, J. S., Chen, W., and Fischer, H.: Quantum Cascade Laser Spectrometry Techniques: A New Trend in Atmospheric Chemistry, Applied Spectroscopy Reviews, 48, 523-559, 2013.

Loubet, B., Cellier, P., Flechard, C., Zurfluh, O., Irvine, M., Lamaud, E., Stella, P., Roche, R., Durand, B., Flura, D., Masson, S., Laville, P., Garrigou, D., Personne, E., Chelle, M., and Castell, J.-F.: Investigating discrepancies in heat, CO2 fluxes and O-3 deposition velocity over maize as measured by the eddy-covariance and the aerodynamic gradient methods, Agricultural and Forest Meteorology, 169, 35-50, 2013.

Loubet, B., Laville, P., Lehuger, S., Larmanou, E., Flechard, C., Mascher, N., Génermont, S., Roche, R., Ferrara, R. M., Stella, P., Personne, E., Durand, B., Decuq, C., Flura, D., Masson, S., Fanucci, O., Rampon, J.-N., Siemens, J., Kindler, R., Schrumpf, M., Gabriele, B., and Cellier, P.: Carbon, nitrogen and Greenhouse gases budgets over a four years crop rotation In northern France, Plant and Soil, 343, 109-137, 2011.

Marr, L. C., Moore, T. O., Klapmeyer, M. E., and Killar, M. B.: Comparison of NOx Fluxes Measured by Eddy Covariance to Emission Inventories and Land Use, Environmental Science & Technology, 47, 1800-1808, 2013.

Martin, R. V., Jacob, D. J., Chance, K., Kurosu, T. P., Palmer, P. I., and Evans, M. J.: Global inventory of nitrogen oxide emissions constrained by space-based observations of NO2 columns, J Geophys Res-Atmos, 108, 2003.

Massman, W. J. and Ibrom, A.: Attenuation of concentration fluctuations of water vapor and other trace gases in turbulent tube flow, Atmospheric Chemistry and Physics, 8, 6245-6259, 2008.

Mauder, M., Foken, T., Clement, R., Elbers, J. A., Eugster, W., Grunwald, T., Heusinkveld, B., and Kolle, O.: Quality control of CarboEurope flux data - Part 2: Inter-comparison of eddy-covariance software, Biogeosciences, 5, 451-462, 2008.

Meixner, F. X.: The surface exchange of nitric oxide, 1997.

Michoud, V., Kukui, A., Camredon, M., Colomb, A., Borbon, A., Miet, K., Aumont, B., Beekmann, M., Durand-Jolibois, R., Perrier, S., Zapf, P., Siour, G., Ait-Helal, W., Locoge, N., Sauvage, S., Afif, C., Gros, V., Furger, M., Ancellet, G., and Doussin, J. F.: Radical budget analysis in a suburban European site during the MEGAPOLI summer field campaign, Atmospheric Chemistry and Physics, 12, 11951-11974, 2012.

Milford, C., Theobald, M. R., Nemitz, E., Hargreaves, K. J., Horvath, L., Raso, J., Daemmgen, U., Neftel, A., Jones, S. K., Hensen, A., Loubet, B., Cellier, P., and Sutton, M. A.: Ammonia fluxes in relation to cutting and fertilization of an intensively managed grassland derived from an inter-comparison of gradient measurements, Biogeosciences, 6, 819-834, 2009.

Min, K. E., Pusede, S. E., Browne, E. C., LaFranchi, B. W., Wooldridge, P. J., and Cohen, R. C.: Eddy covariance fluxes and vertical concentration gradient measurements of NO and NO2 over a ponderosa pine ecosystem: observational evidence for within-canopy chemical removal of NOx, Atmospheric Chemistry and Physics, 14, 5495-5512, 2014.

Minoura, H. and Ito, A.: Observation of the primary NO2 and NO oxidation near the trunk road in Tokyo, Atmospheric Environment, 44, 23-29, 2010.

Muller, J. B. A., Percival, C. J., Gallagher, M. W., Fowler, D., Coyle, M., and Nemitz, E.: Sources of uncertainty in eddy covariance ozone flux measurements made by dry chemiluminescence fast response analysers, Atmospheric Measurement Techniques, 3, 163-176, 2010a.

Muller, M., Graus, M., Ruuskanen, T. M., Schnitzhofer, R., Bamberger, I., Kaser, L., Titzmann, T., Hortnagl, L., Wohlfahrt, G., Karl, T., and Hansel, A.: First eddy covariance flux measurements by PTR-TOF, Atmospheric Measurement Techniques, 3, 387-395, 2010b.

Murphy, J. G., Day, D. A., Cleary, P. A., Wooldridge, P. J., Millet, D. B., Goldstein, A. H., and Cohen, R. C.: The weekend effect within and downwind of Sacramento - Part 1: Observations of ozone, nitrogen oxides, and VOC reactivity, Atmospheric Chemistry and Physics, 7, 5327-5339, 2007.

Oikawa, P. Y., Ge, C., Wang, J., Eberwein, J. R., Liang, L. L., Allsman, L. A., Grantz, D. A., and Jenerette, G. D.: Unusually high soil nitrogen oxide emissions influence air quality in a high-temperature agricultural region, Nature communications, 6, 8753, 2015.

Oswald, R., Behrendt, T., Ermel, M., Wu, D., Su, H., Cheng, Y., Breuninger, C., Moravek, A., Mougin, E., Delon, C., Loubet, B., Pommerening-Röser, A., Sörgel, M., Pöschl, U., Hoffmann, T., Andreae, M. O., Meixner, F. X., and Trebs, I.: HONO Emissions from Soil Bacteria as a Major Source of Atmospheric Reactive Nitrogen, Science, 341, 1233-1235, 2013.

Pape, L., Ammann, C., Nyfeler-Brunner, A., Spirig, C., Hens, K., and Meixner, F. X.: An automated dynamic chamber system for surface exchange measurement of non-reactive and reactive trace gases of grassland ecosystems, Biogeosciences, 6, 405-429, 2009.

Park, J. H., Fares, S., Weber, R., and Goldstein, A. H.: Biogenic volatile organic compound emissions during BEARPEX 2009 measured by eddy covariance and flux-gradient similarity methods, Atmospheric Chemistry and Physics, 14, 231-244, 2014.

Peltola, O., Hensen, A., Helfter, C., Belelli Marchesini, L., Bosveld, F. C., van den Bulk, W. C. M., Elbers, J. A., Haapanala, S., Holst, J., Laurila, T., Lindroth, A., Nemitz, E., Röckmann, T., Vermeulen, A. T., and Mammarella, I.: Evaluating the performance of commonly used gas analysers for methane eddy covariance flux measurements: the InGOS inter-comparison field experiment, Biogeosciences, 11, 3163-3186, 2014.

Penuelas, J., Asensio, D., Tholl, D., Wenke, K., Rosenkranz, M., Piechulla, B., and Schnitzler, J. P.: Biogenic volatile emissions from the soil, Plant Cell and Environment, 37, 1866-1891, 2014.

Personne, E., Loubet, B., Herrmann, B., Mattsson, M., Schjoerring, J. K., Nemitz, E., Sutton, M. A., and Cellier, P.: SURFATM-NH3: a model combining the surface energy balance and bi-directional exchanges of ammonia applied at the field scale, Biogeosciences, 6, 1371-1388, 2009.

Plake, D., Soergel, M., Stella, P., Held, A., and Trebs, I.: Influence of meteorology and anthropogenic pollution on chemical flux divergence of the NO-NO2-O-3 triad above and within a natural grassland canopy, Biogeosciences, 12, 945-959, 2015.

Reeser, D. I., Jammoul, A., Clifford, D., Brigante, M., D'Anna, B., George, C., and Donaldson, D. J.: Photoenhanced Reaction of Ozone with Chlorophyll at the Seawater Surface, Journal of Physical Chemistry C, 113, 2071-2077, 2009.

Remde, A., Slemr, F., and Conrad, R.: Microbial-Production and Uptake of Nitric-Oxide in Soil, Fems Microbiol Ecol, 62, 221-230, 1989.

Rummel, U., Ammann, C., Gut, A., Meixner, F. X., and Andreae, M. O.: Eddy covariance measurements of nitric oxide flux within an Amazonian rain forest, J Geophys Res-Atmos, 107, 2002.

Seinfeld, J. H. and Pandis, S. N.: Atmospheric chemistry and physics. From air pollution to climate change, Wiley-Interscience, 2016.

Sintermann, J., Spirig, C., Jordan, A., Kuhn, U., Ammann, C., and Neftel, A.: Eddy covariance flux measurements of ammonia by high temperature chemical ionisation mass spectrometry, Atmos. Meas. Tech., 4, 599-616, 2011.

Skiba, U., Drewer, J., Tang, Y. S., van Dijk, N., Helfter, C., Nemitz, E., Famulari, D., Cape, J. N., Jones, S. K., Twigg, M., Pihlatie, M., Vesala, T., Larsen, K. S., Carter, M. S., Ambus, P., Ibrom, A., Beier, C., Hensen, A., Frumau, A., Erisman, J. W., Brueggemann, N., Gasche, R., Butterbach-Bahl, K., Neftel, A., Spirig, C., Horvath, L., Freibauer, A., Cellier, P., Laville, P., Loubet, B., Magliulo, E., Bertolini, T., Seufert, G., Andersson, M., Manca, G., Laurila, T., Aurela, M., Lohila, A., Zechmeister-Boltenstern, S., Kitzler, B., Schaufler, G., Siemens, J., Kindler, R., Flechard, C., and Sutton, M. A.: Biosphere-atmosphere exchange of reactive nitrogen and greenhouse gases at the NitroEurope core flux measurement sites: Measurement strategy and first data sets, Agriculture Ecosystems & Environment, 133, 139-149, 2009.

Springs, M., Wells, J. R., and Morrison, G. C.: Reaction rates of ozone and terpenes adsorbed to model indoor surfaces, Indoor Air, 21, 319-327, 2011.

Stella, P., Kortner, M., Ammann, C., Foken, T., Meixner, F. X., and Trebs, I.: Measurements of nitrogen oxides and ozone fluxes by eddy covariance at a meadow: evidence for an internal leaf resistance to NO2, Biogeosciences, 10, 5997-6017, 2013.

Stella, P., Loubet, B., Lamaud, E., Laville, P., and Cellier, P.: Ozone deposition onto bare soil: a new parameterisation, Agricultural and Forest Meteorology, 151, 669-681, 2011.

Stella, P., Loubet, B., Laville, P., Lamaud, E., Cazaunau, M., Laufs, S., Bernard, F., Grosselin, B., Mascher, N., Kurtenbach, R., Mellouki, A., Kleffmann, J., and Cellier, P.: Comparison of methods for the determination of NO-O-3-NO2 fluxes and chemical interactions over a bare soil, Atmospheric Measurement Techniques, 5, 1241-1257, 2012.

Stokes, G. Y., Buchbinder, A. M., Gibbs-Davis, J. M., Scheidt, K. A., and Geiger, F. M.: Heterogeneous Ozone Oxidation Reactions of 1-Pentene, Cyclopentene, Cyclohexene, and a Menthenol Derivative Studied by Sum Frequency Generation, Journal of Physical Chemistry A, 112, 11688-11698, 2008.

Toenges-Schuller, N., Stein, O., Rohrer, F., Wahner, A., Richter, A., Burrows, J. P., Beirle, S., Wagner, T., Platt, U., and Elvidge, C. D.: Global distribution pattern of anthropogenic nitrogen oxide emissions: Correlation analysis of satellite measurements and model calculations, J Geophys Res-Atmos, 111, 2006.

Trebs, I., Bohn, B., Ammann, C., Rummel, U., Blumthaler, M., Koenigstedt, R., Meixner, F. X., Fan, S., and Andreae, M. O.: Relationship between the NO2 photolysis frequency and the solar global irradiance, Atmospheric Measurement Techniques, 2, 725-739, 2009.

Trebs, I., Mayol-Bracero, O. L., Pauliquevis, T., Kuhn, U., Sander, R., Ganzeveld, L., Meixner, F. X., Kesselmeier, J., Artaxo, P., and Andreae, M. O.: Impact of the Manaus urban plume on trace gas mixing ratios near the surface in the Amazon Basin: Implications for the NO-NO2-O-3 photostationary state and peroxy radical levels, J Geophys Res-Atmos, 117, 2012.

Williams, E. J. and Fehsenfeld, F. C.: Measurement of Soil-Nitrogen Oxide Emissions at 3 North-American Ecosystems, J Geophys Res-Atmos, 96, 1033-1042, 1991.

Wolfe, G. M., Thornton, J. A., McKay, M., and Goldstein, A. H.: Forest-atmosphere exchange of ozone: sensitivity to very reactive biogenic VOC emissions and implications for in-canopy photochemistry, Atmospheric Chemistry and Physics, 11, 7875-7891, 2011.

Wolfe, G. M., Thornton, J. A., Yatavelli, R. L. N., McKay, M., Goldstein, A. H., LaFranchi, B., Min, K. E., and Cohen, R. C.: Eddy covariance fluxes of acyl peroxy nitrates (PAN, PPN and MPAN) above a Ponderosa pine forest, Atmospheric Chemistry and Physics, 9, 615-634, 2009.

Biogeosciences Discuss., doi:10.5194/bg-2016-199, 2016
Manuscript under review for journal Biogeosciences
Published: 29 June 2016

Yienger, J. J. and Levy, H.: Empirical-Model of Global Soil-Biogenic Nox Emissions, J Geophys Res-Atmos, 100, 11447-11464, 1995.

760

Biogeosciences Discuss., doi:10.5194/bg-2016-199, 2016
Manuscript under review for journal Biogeosciences
Published: 29 June 2016

Figures

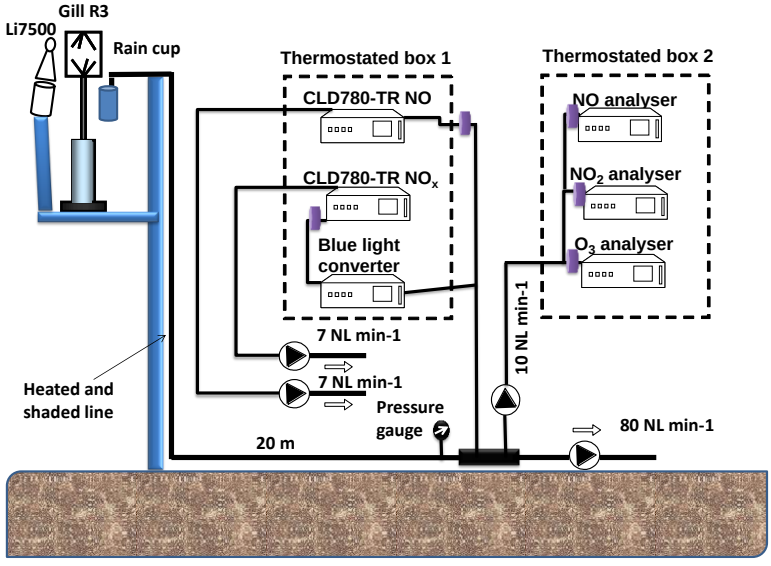

765 **Figure 1. Simplified sketch of the field and instrument setup to measure EC fluxes. Gill R3 is the ultrasonic anemometer, Li7500 is the open path infrared CO_2 and H_2O gas analyser, the rain cup is the air sampler for NO and NO_2 detection. CLD780-TR NO and NOx are the fast-response NO analysers (Ecophysics) operating in parallel, one connected to a BLC measuring NO + αNO_2. The NO, NO_2, and O_3 slow analysers (ThermoScientific, Waltham, USA) are placed behind a Teflon pump ensuring atmospheric pressure at the inlet. A large pallet pump ensured a flow rate**
770 **of 80 NL min^{-1} in the heated inlet line. Teflon filters (1µm) were installed at the front of the instrument inlets (purple cylinders).**

Biogeosciences Discuss., doi:10.5194/bg-2016-199, 2016
Manuscript under review for journal Biogeosciences
Published: 29 June 2016

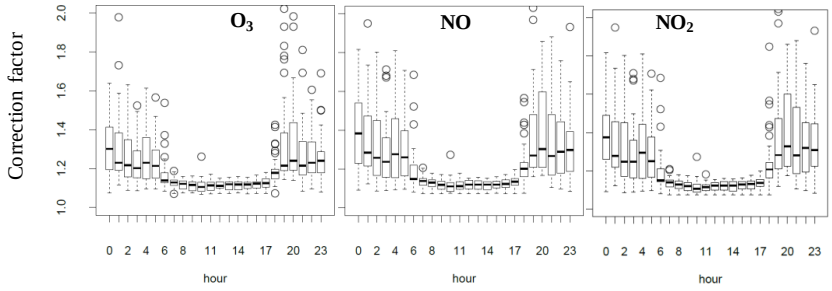

775 **Figure 2. Hourly averaged high frequency loss correction factors for O_3, NO and NO_2 over the 15 August-7 September period determined with the in situ ogive method. The corrected flux equals the measured flux multiplied by the correction factor. Black bars are medians, boxes show the interquartile, error-bars show the minimum and maximum of the whisker and empty dots shows the outliers.**

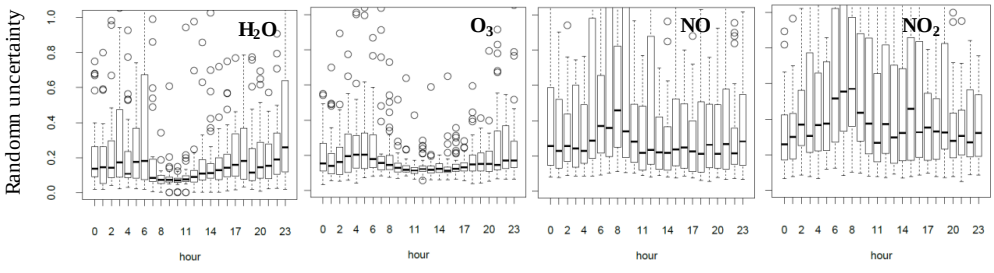

780 **Figure 3. Daily variations of the ratio of the random uncertain to the flux for H_2O, O_3, NO and NO_2 during august 2012 (15 August to 9 September). Black bars are medians, boxes show the interquartile, error-bars show the minimum and maximum of the whisker and empty dots shows the outliers.**

785

Biogeosciences Discuss., doi:10.5194/bg-2016-199, 2016
Manuscript under review for journal Biogeosciences
Published: 29 June 2016

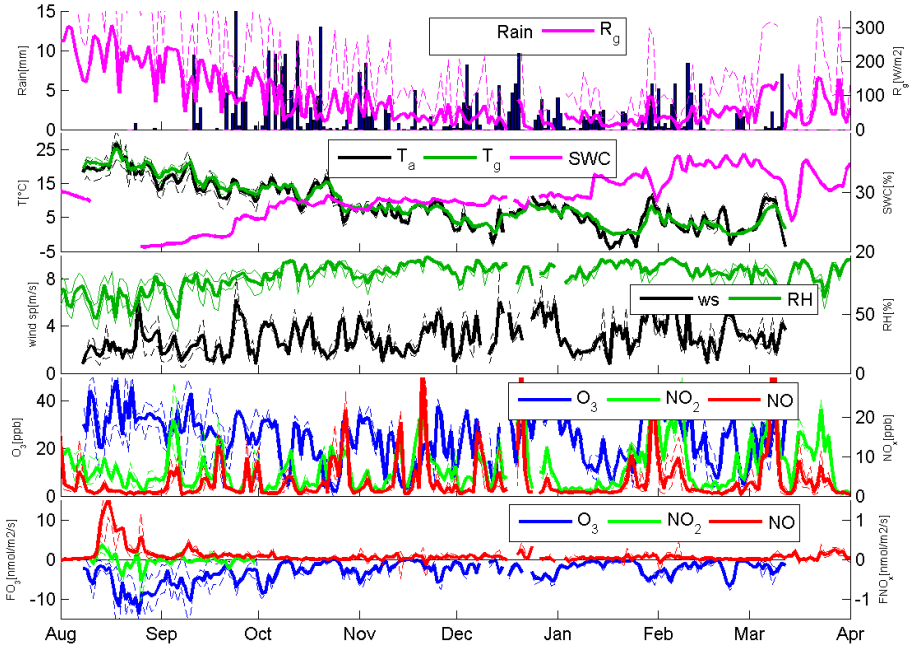

Figure 4. Meteorological and soil conditions (daily averages, sums for rainfall), NO, NO_2 and O_3 mixing ratios and fluxes during the entire measurement period from 07/08/2012 to 13/03/2013 at the Grignon field site. Averages for night-time and daytime are also given as dotted lines. R_g is the global radiation, T_a and T_g the air and ground temperature, SWC the soil water content, ws the wind speed, RH the air relative humidity.

Biogeosciences Discuss., doi:10.5194/bg-2016-199, 2016
Manuscript under review for journal Biogeosciences
Published: 29 June 2016

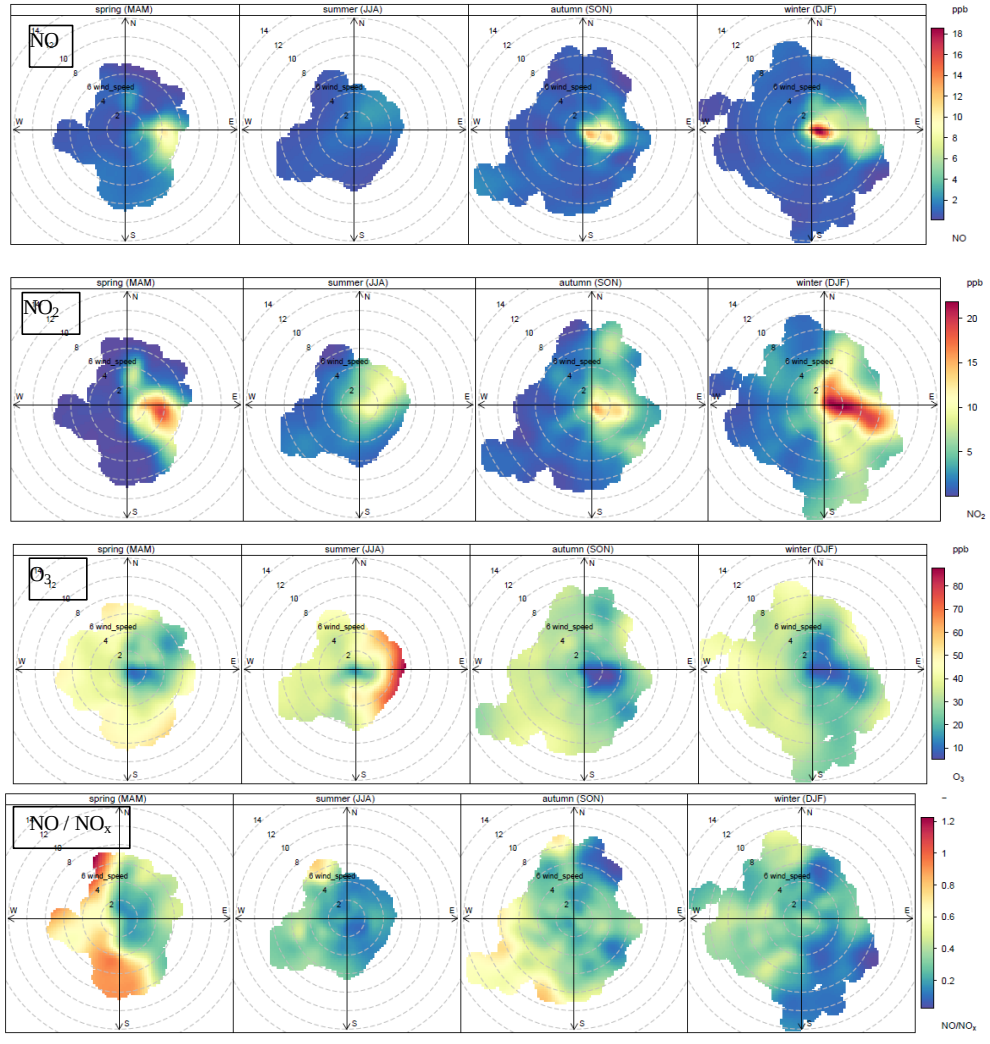

795

Figure 5. Angular distribution (wind roses) of wind direction, wind speed, NO, O_3 and NO_2 mixing ratios over the whole experimental period separated by seasons measured at the Grignon field site from 07/08/2012 to 13/03/2013.

800

Biogeosciences Discuss., doi:10.5194/bg-2016-199, 2016
Manuscript under review for journal Biogeosciences
Published: 29 June 2016

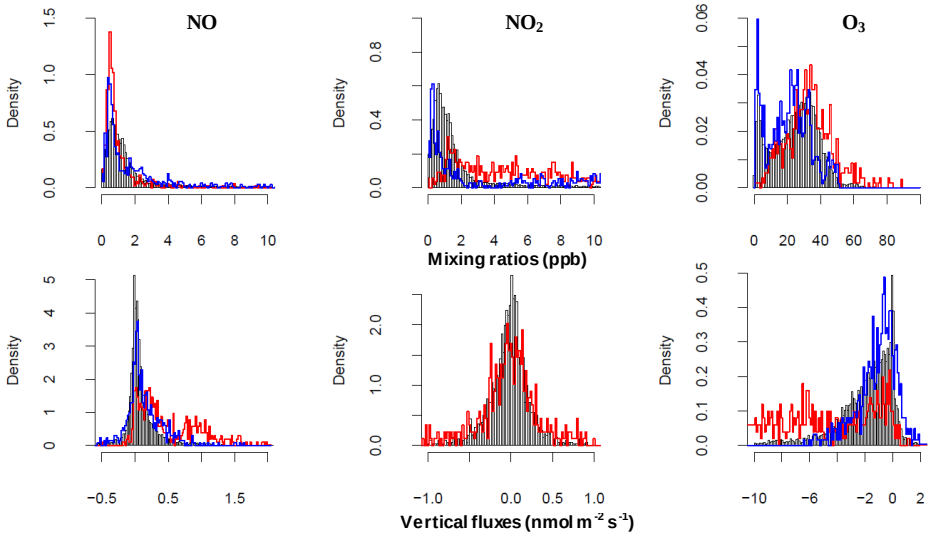

805

Figure 6. Histograms of (a) O_3, NO and NO_2 mixing ratios and (b) fluxes (black), following organic spreading (red) and mineral fertilisation (blue) measured at the Grignon field site. In y-axes are shown the density which is the frequency divided by the number of elements.

810

Biogeosciences Discuss., doi:10.5194/bg-2016-199, 2016
Manuscript under review for journal Biogeosciences
Published: 29 June 2016

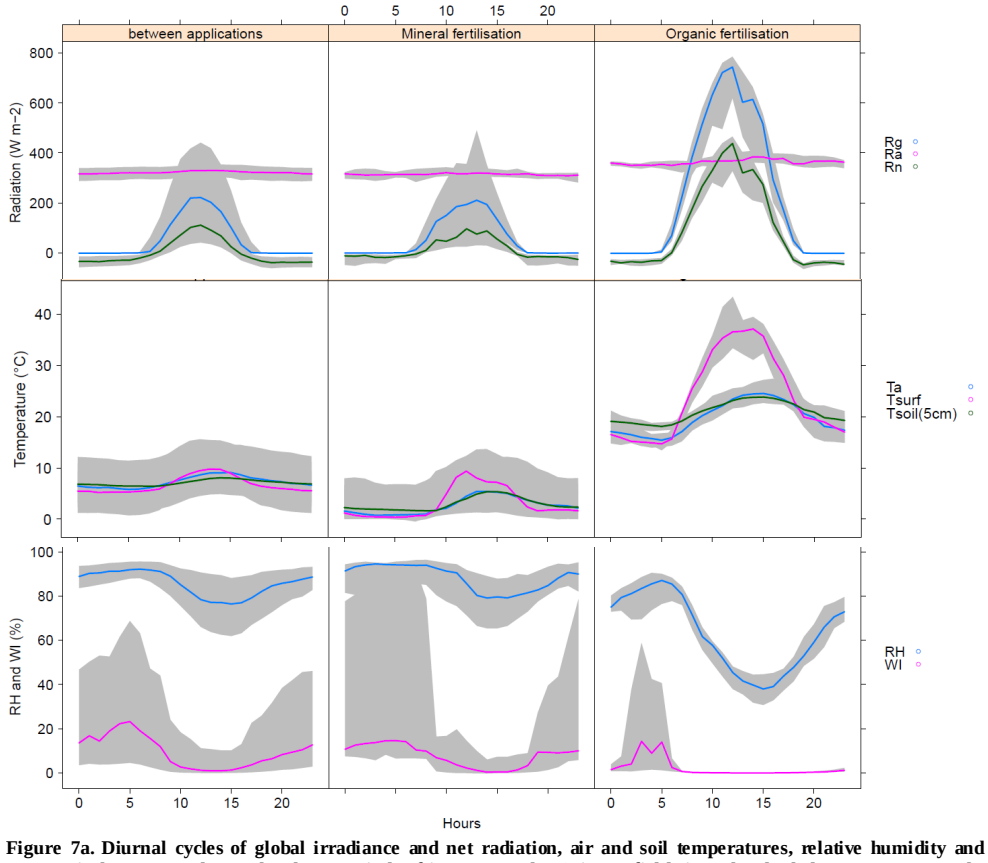

Figure 7a. Diurnal cycles of global irradiance and net radiation, air and soil temperatures, relative humidity and wetness index averaged over the three periods of interest at the Grignon field site. The shaded areas represent the interquartile range.

Biogeosciences Discuss., doi:10.5194/bg-2016-199, 2016
Manuscript under review for journal Biogeosciences
Published: 29 June 2016

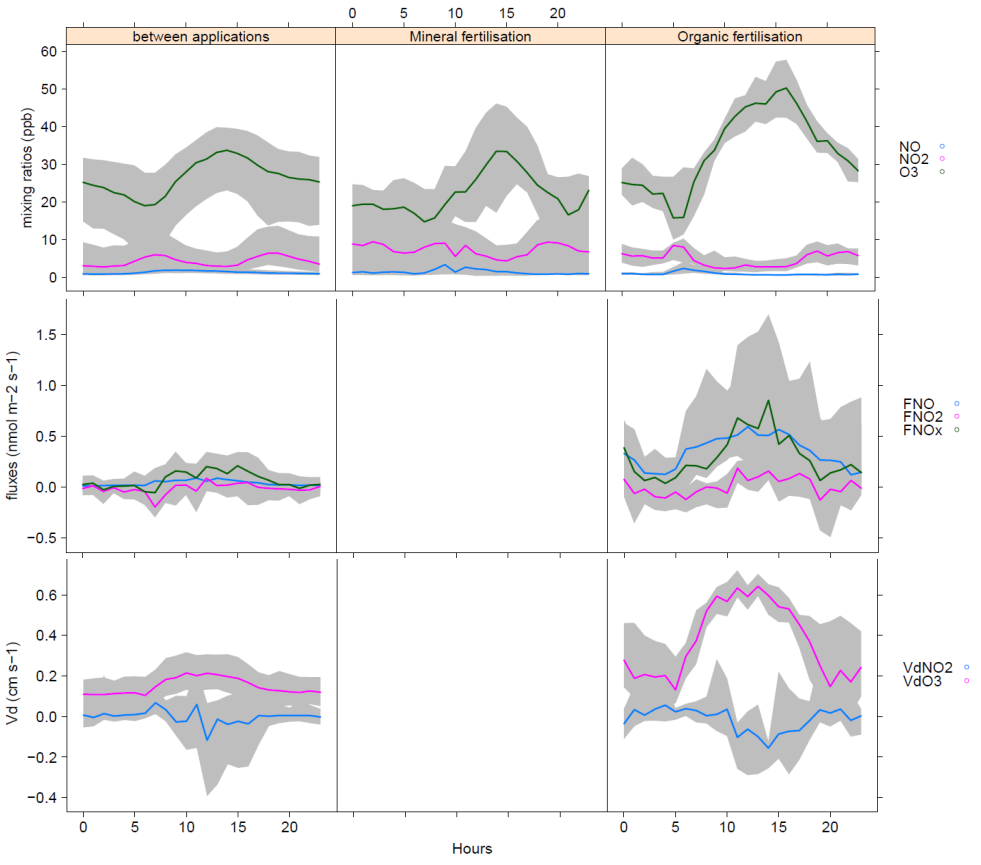

Figure 7b. Diurnal cycles of NO, NO_2 and O_3 mixing ratios and fluxes as well as the deposition velocities of NO_2 and O_3, averaged over the three periods of interest at the Grignon field site. The shaded areas represent the interquartile range.

Biogeosciences Discuss., doi:10.5194/bg-2016-199, 2016
Manuscript under review for journal Biogeosciences
Published: 29 June 2016

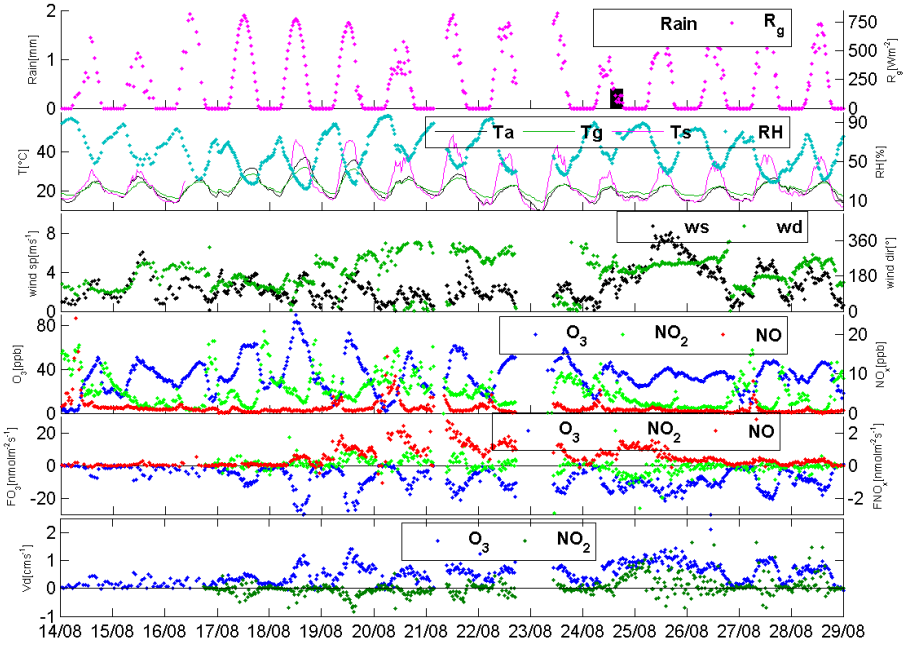

Figure 8. Meteorological variables and NO_x-O_3 mixing ratios and fluxes measured during the period 14/08/12 to 29/08/12 at the Grignon fieldsite. Ticks on the x-axis correspond to midnight.

830

Biogeosciences Discuss., doi:10.5194/bg-2016-199, 2016
Manuscript under review for journal Biogeosciences
Published: 29 June 2016

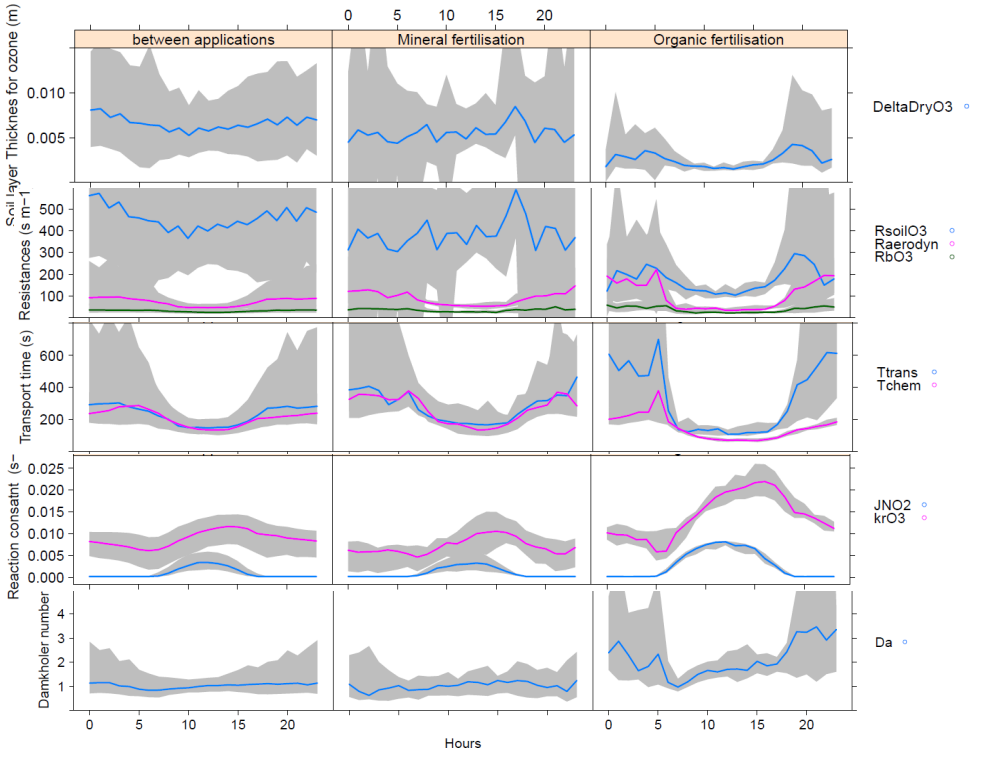

Figure 9. Diurnal cycles of the O_3 penetration depth in the soil (DeltaDryO3), the aerodynamic (Ra), boundary layer (RbO3) and soil resistances (RsoilO3) for O_3, the chemical reaction time τ_{chem} and transport time τ_{trans}, the chemical reaction rates for NO_2 photolysis J_{NO2} and NO depletion by O_3 ($k_r \times [O_3]$), and the Damköhler number (Da), averaged over the periods of interest at the Grignon field site. The shaded areas represent the interquartile range.

Biogeosciences Discuss., doi:10.5194/bg-2016-199, 2016
Manuscript under review for journal Biogeosciences
Published: 29 June 2016

840

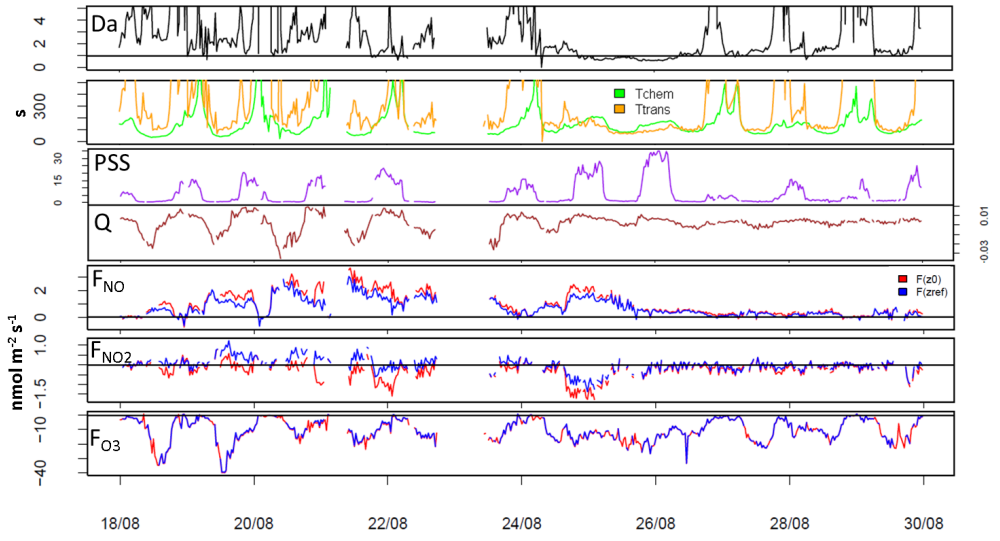

Figure 10. Half-hourly values of photo-stationary state ratio (PSS) and Q = k_r [NO][O_3] - J_{NO2}[NO_2]; chemistry and transport timescales (Tchem and Ttrans) and Damköhler number (Da); measured NO, NO_2 and O_3 fluxes and surface fluxes as computed by assuming a logarithmic flux divergence profile (F_{NO}, F_{NO2} and F_{O3}) at the Grignon field site.